Available online at www.sciencedirect.com
SCIENCE DIRECT
Journal of the European Ceramic Society 26 (2006) 435–441
www.elsevier.com/locate/jeurceramsoc

Atomic structures and formation mechanism of boron nitride nanotubes and nanohorns synthesized by arc-melting LaB_6 powders

Atsushi Nishiwaki, Takeo Oku *

Institute of Scientific and Industrial Research, Osaka University, Mihogaoka 8-1, Ibaraki, Osaka 567-0047, Japan

Available online 10 August 2005

Abstract

Boron nitride (BN) nanotubes and nanohorns with various tip structures were synthesized by arc-melting LaB_6 powders. Atomic structure models and formation mechanism for BN nanotubes and nanohorns were proposed from high-resolution electron microscopy (HREM), energy dispersive X-ray spectroscopy (EDX), molecular mechanics calculations (MM2) and thermodynamic calculation. The present work indicates that lanthanum would be a key catalytic material to produce the BN nanostructures.

Keywords: Powders-solid state; Nanotubes; Electron microscopy; Nanocomposites; Nitrides

1. Introduction

Carbon-based nanocage structures, such as fullerene clusters, nanotubes, nanopolyhedra, cones, cubes and onions, have great potential for studying materials of low dimensions in an isolated environment.[1–3] Especially, carbon nanohorns as a novel type of carbon nanotubes are expected as catalyst electrode materials for next-generation fuel cells, which separate hydrogen and electrons from methanol.[4–9] Boron nitride (BN) nanostructured materials with a bandgap energy of ∼6 eV and non-magnetism are also expected to show various electronic, optical and magnetic properties such as Coulomb blockade, photoluminescence, and supermagnetism.[3,10–12]

Recently, several studies have been reported on BN nanomaterials such as BN nanotubes,[13–16] BN nanocapsules[3,10,15] and BN nanoparticles,[17,18] which are expected to be useful as electronic devices, high heat-resistance semiconductors and insulator lubricants. Some BN nanocage clusters have been predicted theoretically,[19] and BN clusters with sizes of ∼1 nm were observed by high-resolution electron microscopy (HREM)[3,10,20] and mass spectrometry.[21,22] BN nanohorns as a novel type of BN nanotubes were also reported by HREM image.[23,24]

The purpose of the present work is to synthesize BN nanotubes and nanohorns, and to investigate the atomic structures and formation mechanism by HREM, electron dispersive X-ray spectroscopy (EDX), molecular mechanics calculations (MM2) and thermodynamic calculation. To synthesize BN nanotubes and nanohorns with various tip structure, LaB_6 powder was selected for arc-melting, which is a useful catalysis for BN nanotube synthesis.[3] The present study will give us a guideline for designing and synthesis of the BN nanotubes and nanohorns, which are expected as future nanoscale devices.

2. Experimental procedures

The LaB_6 powder (4 g, 99%, Kojundo Chemical Lab. Co. Ltd.) was set on a copper mold in an electric-arc furnace, which was evacuated down to 1.0×10^{-3} Pa. After introducing a mixed gas of Ar (0.025 MPa) and N_2 (0.025 MPa), arc-melting was applied to the samples at an accelerating voltage of 200 V and an arc current of 125 A for 10 s. Arc-melting was performed with a vacuum arc-melting furnace (NEV-AD03, Nisshin Engineering Co. Ltd.). Samples for

* Corresponding author. Tel.: +81 6 6879 8521; fax: +81 6 6879 8522.
E-mail address: oku@sanken.osaka-u.ac.jp (T. Oku).

0955-2219/$ – see front matter © 2005 Elsevier Ltd. All rights reserved.
doi:10.1016/j.jeurceramsoc.2005.06.030

HREM observation were prepared by dispersing the materials on holey carbon grids. HREM observation was performed with a 300 kV electron microscope (JEM-3000F). To confirm the formation of BN nanomaterials, EDX analysis was performed by the EDAX system.

Basic structure models for BN nanotubes, nanohorns and BN cluster were constructed by CS Chem3D (CambridgeSoft). For stability calculations, structural optimization of the BN nanostructures were performed by molecular mechanics calculations. Standard reaction enthalpy (ΔH_r°) and standard reaction Gibbs energy (ΔG_r°) were calculated by chemical reaction and equilibrium software (HSC Chemistry 4.0, Outokumpu Research, Finland).

3. Results and discussion

Fig. 1 is HREM image of multi-walled BN nanotubes synthesized by an arc-melting method. {0 0 2} layers of BN are clearly observed in these images. Tips of BN nanotubes of Fig. 1(a) and (b) are flat and horn type, respectively. The tip of BN nanotube is choked up by an amorphous phase, as

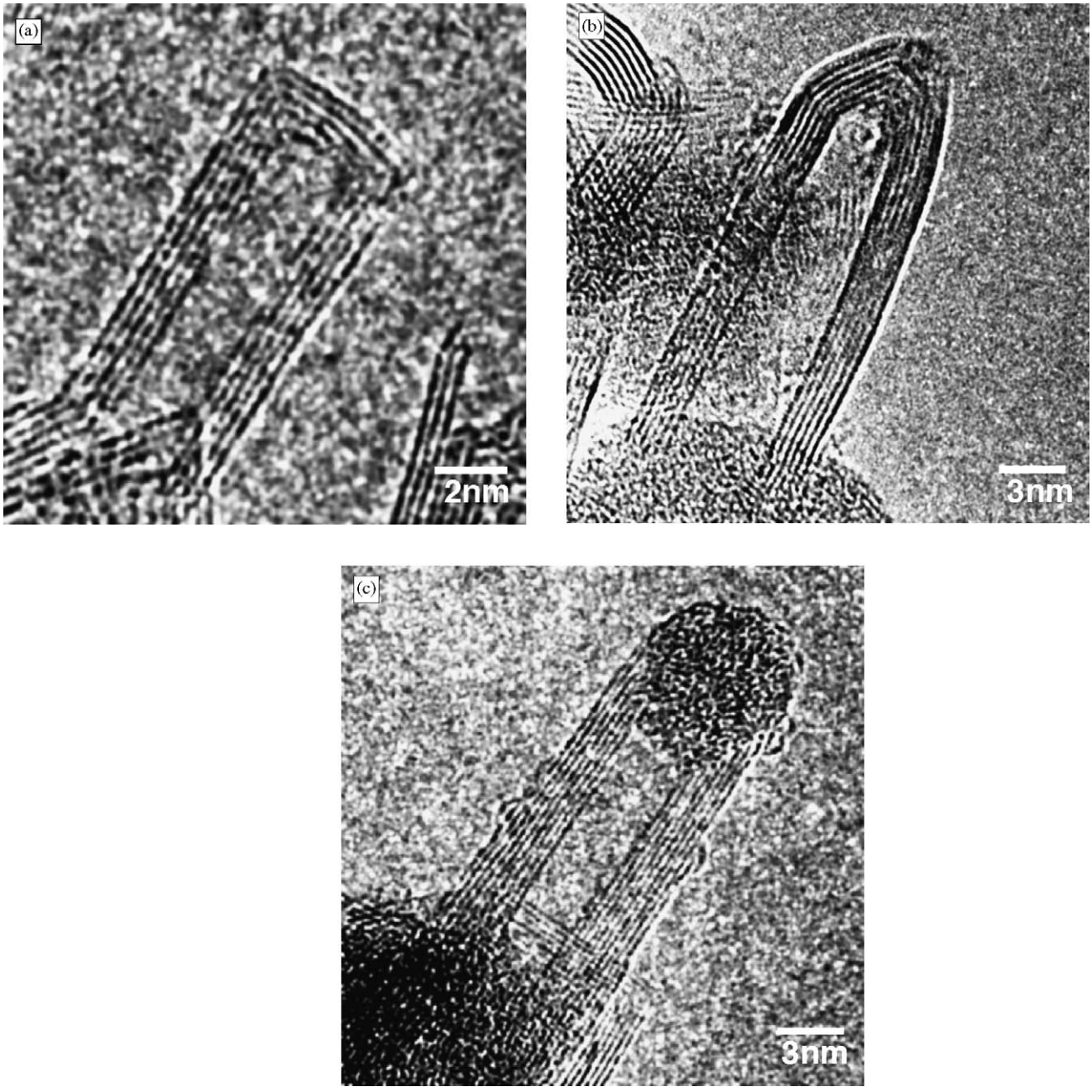

Fig. 1. HREM images of BN nanotubes with (a) flat and (b) horn structure; (c) BN nanotube with amorphous particle.

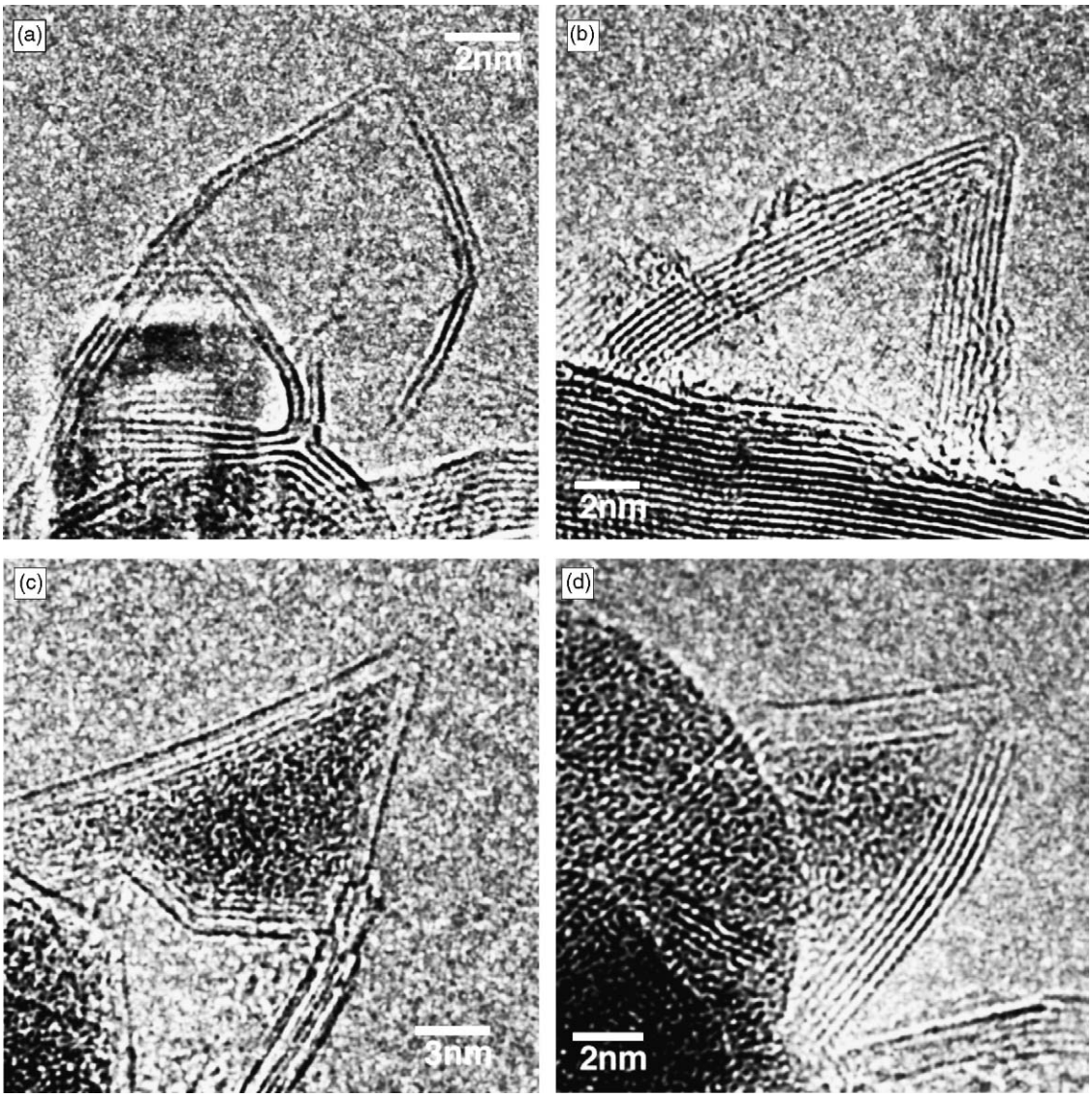

Fig. 2. HREM images of BN nanohorns with (a), (b) a hollow structure and (c, d) amorphous phase.

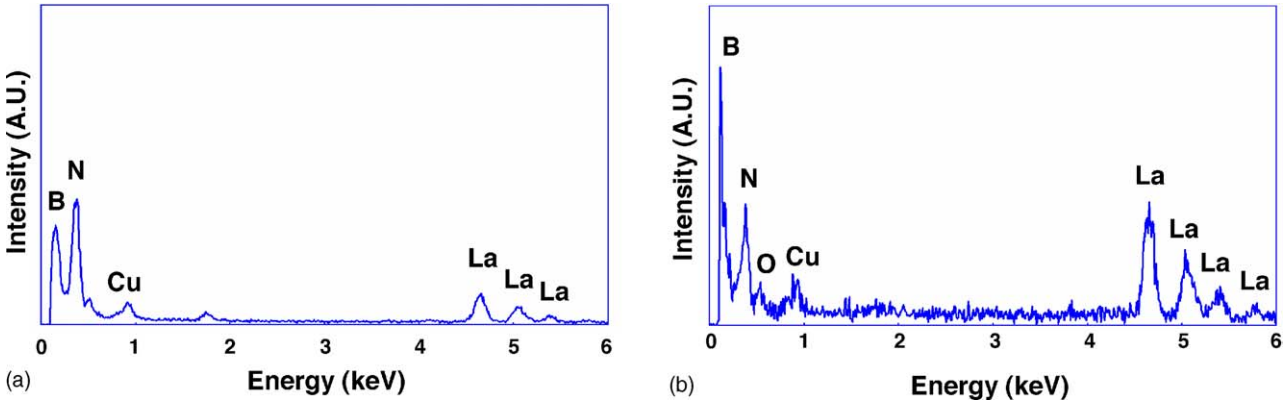

Fig. 3. EDX spectrum of BN nanohorns with (a) a hollow structure and (b) amorphous phase.

shown in Fig. 1(c). On the other hand, amorphous phases are observed at the root of BN nanotubes in Fig. 1(b) and (c), respectively.

Fig. 2 is HREM image of multi-walled BN nanohorns synthesized by the present method. Tip angles of BN nanohorns of Fig. 2(a), and (b) are ∼80° and ∼60°, respectively. Tip angles of BN nanohorns with amorphous phase of Fig. 2(c) and (d) are both ∼60°. Since the distortion of tips of BN nanohorns is very large, the structure may not be completely perfect, which results in the vague contrast at the tips.

EDX spectra of BN nanohorns with a hollow and an amorphous phase are shown in Fig. 3(a) and (b), respectively. Both graphs are normalized by nitrogen peaks. Fig. 3(a) shows boron and nitrogen peaks, and Fig. 3(b) shows peaks of lan-

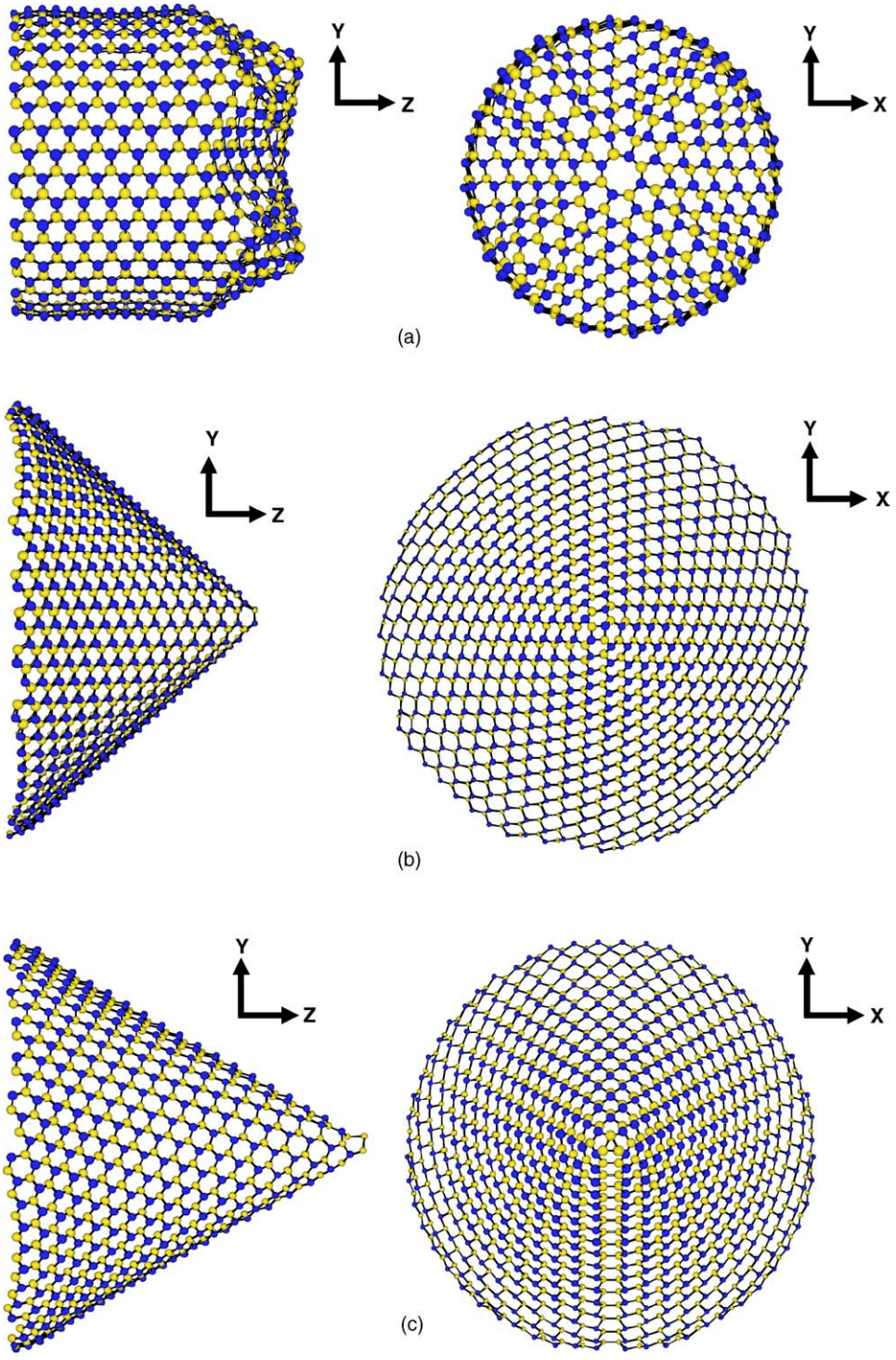

Fig. 4. Structure models for (a) BN nanotube with flat tip, and BN nanohorns with tip angles of (b) 84° and (c) 60°, respectively.

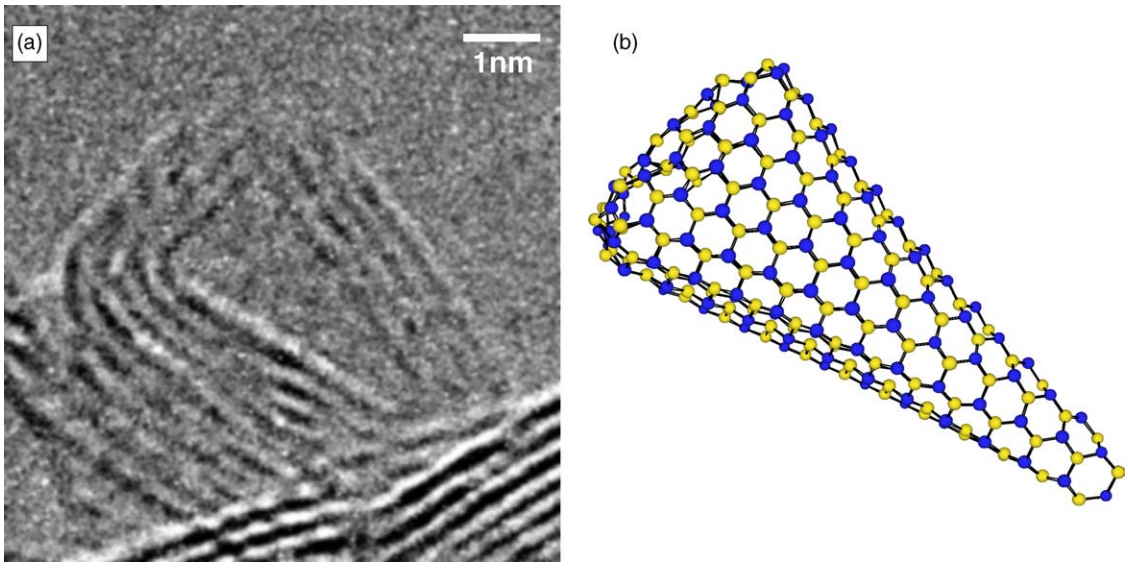

Fig. 5. (a) HREM image and (b) structure model of BN cluster with trigonal shape.

thanum in addition to peaks of boron, nitrogen, oxygen and copper. Weak peaks of copper are due to the HREM grid. The composition ratio of B:N:La in Fig. 3(a) and (b) are calculated to be 43.9:45.4:10.7 and 34.0:27.5:38.5, respectively. Since the composition ratio of B:N in Fig. 3(a) is almost ∼1.0, these B and N peaks are believed to be detected from BN layers. If the composition ratio of BN in Fig. 3(b) is assumed to be 1.0, composition of the amorphous phases would be $LaB_{0.17}$, which indicates that most of the amorphous phases were lanthanum. Amorphous phases observed at the root of BN nanotubes and nanohorns in Figs. 1(b) and (c), 2(a), (d), and (e) would be starting points of BN growth.

From the results of HREM observation of Figs. 1(a) and 2, structure models for BN nanohorns were proposed, as shown in Fig. 4. Structure models of Fig. 4(a)–(c) are $B_{480}N_{480}$ nanotube, $B_{535}N_{535}$ nanohorn and $B_{557}N_{541}$ nanohorn, respectively. Four and one tetragonal BN rings are introduced for the model in Fig. 4(a) and (b), respectively. Since a trigonal BN ring is introduced for a model in Fig. 4(c), the structure model of Fig. 4(c) has some B–B bonds. The difference of tip angles in observations of Fig. 2 and calculations in Fig. 4 would be due to the lattice defect. The minimum numbers of BN layers in nanohorns synthesized by the present work is two,

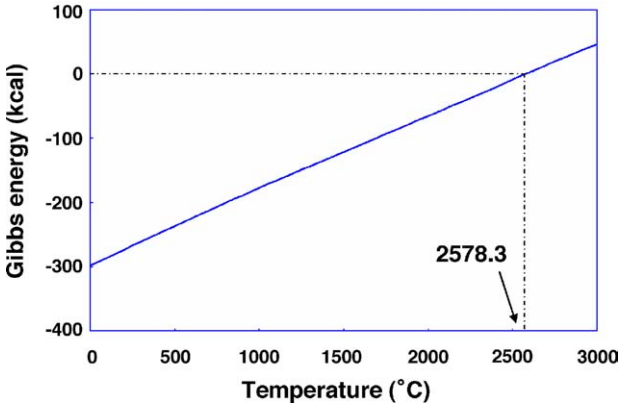

Fig. 6. Temperature dependence of Gibbs energy calculated based on Eq. (1).

which would be due to stacking stability with two elements of boron and nitrogen. The double-walled model of $B_{535}N_{535}$ and $B_{557}N_{541}$ nanohorns with 84° and 60° were constructed, and total energies for $B_{480}N_{480}$, $B_{535}N_{535}$, $B_{557}N_{541}$ and double-walled BN nanohorns were investigated by molecular mechanics calculation, as summarized in Table 1. Distance

Table 1
Calculated total energies of BN nanotube and nanohorns

Structure types	Nanotube	Nanohorn			
	$B_{480}N_{480}$	$B_{535}N_{535}$	$B_{1070}N_{1070}$	$B_{557}N_{541}$	$B_{1114}N_{1082}$
Tip angle (°)		84	84	60	60
Number of layers	1	1	2	1	2
Number of trigonal BN rings	0	0	0	1	1
Number of tetragonal BN rings	4	1	1	0	0
Number of octagonal BN rings	1	0	0	0	0
Total energy (kcal/mol)	1259	1059	1211	1182	1495
Total energy (kcal/mol atom)	1.311	0.9897	0.5659	1.077	0.6808

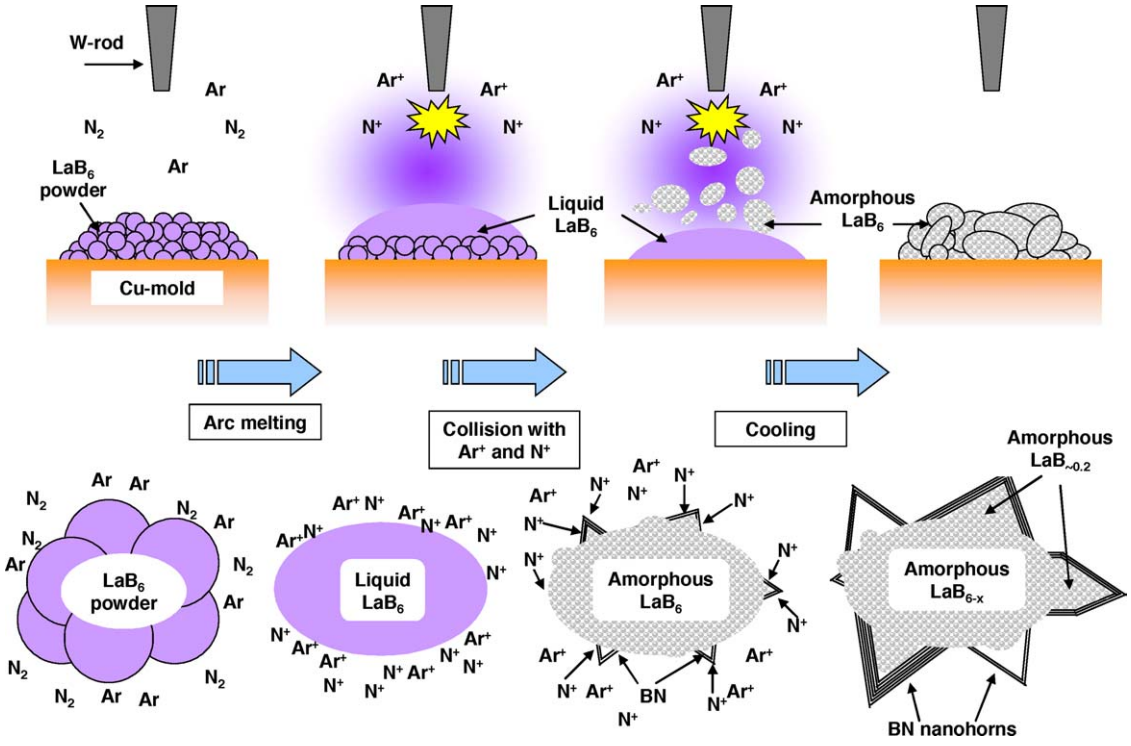

Fig. 7. Schematic illustration of the formation mechanism of BN nanohorns.

between BN layers of the double-walled BN nanohorn structures in a HREM image was measured to be ∼0.35 nm, and the basic structure model was constructed based on it. After molecular mechanics calculation, the layer distances were optimized as 0.38 nm. Comparing total energies of BN nanotube and single-walled BN nanohorns, BN nanohorns shows a lower energy per mol atom than that of BN nanotube. Higher total energy of BN nanotube would be due to the distortion of four tetragonal BN rings of the tip. Comparing total energies of BN nanohorns with 84° and 60°, BN nanohorns with 85° shows a lower energy per mol atom than that of BN nanohorn with 60°. Higher total energy of BN nanohorn with 60° would be due to the distortion of one trigonal BN ring of the tip and some B–B bonds. In addition, total energies per mol atom of double-walled BN nanohorns with 84° and 60° were reduced by stacking of BN nanohorn structure, and it is believed that the structure of BN multi-layered nanohorns would be stabilized by stacking hexagonal BN ring networks.

Fig. 5(a) is a HREM image of a BN cluster with trigonal shape synthesized at the same time. A structure model of BN cluster with trigonal shape was proposed, as shown in Fig. 5(b). Four tetragonal, one pentagonal and one heptagonal BN rings are introduced for the model in Fig. 5(b).

In the present work, the formation process was proposed, as a following equation.

$$LaB_6 + 3N_2(g) \rightarrow La + 6BN \quad (1)$$

For the Eq. (1), the Gibbs free energy (ΔG_r°) was minus at temperatures below 2578.3 °C. Temperature dependence of Gibbs energy calculated based on the Eq. (1) is shown in Fig. 6, which indicates the reaction of BN formation would occur below 2578.3 °C spontaneously.

Schematic illustration of the formation mechanism of BN nanohorns is shown in Fig. 7. First, argon and nitrogen ions are produced by the arc discharge. LaB_6 powder is melted by the arc-melting, and liquid LaB_6 would be cooled in argon and nitrogen ion gas. In this process, liquid LaB_6 would become an amorphous phase, and BN layers would be formed at the surface of amorphous LaB_6. Since boron in amorphous LaB_6 is used for BN layer formation, amorphous phases close to BN layers would be become La-rich $LaB_{\sim 0.2}$, as shown in EDX results. Center of amorphous LaB_6 particles would be become LaB_{6-x} because boron in amorphous LaB_6 was used for BN formation. Lanthanum atoms would act as a catalyst for possible starting points of growth of BN nanotubes and nanohorns, and the amorphous phase worked as a key catalytic material to produce the BN nanostructures.

4. Conclusion

Various BN nanostructures were synthesized by an arc-melting of LaB_6 powder in N_2/Ar mixture gas. Atomic structure models for the BN nanotubes, nanohorns and BN cluster with trigonal shape were proposed from HREM observation and molecular mechanics calculations. Multi-walled structures with trigonal and tetragonal BN ring networks would be stabilized by stacking BN nanohorns. The EDX results showed the amorphous phases in the BN nanohorns were

$LaB_{\sim 0.2}$, and the formation mechanism was proposed from the structure analysis and thermodynamic calculation.

References

1. Kroto, H. W., Heath, J. R., O'Brien, S. C., Curl, R. F. and Smalley, R. E., C_{60}: Backminsterfullerence. *Nature*, 1985, **318**, 162–163.
2. Iijima, S., Helical microtubes of graphitec carbon. *Nature*, 1991, **354**, 56–58.
3. Oku, T., Kuno, M., Kitahara, H. and Narita, I., Formation, atomic structures and properties of boron nitride and carbon nanocage fullerene. *Int. J. Inorg. Mater.*, 2001, **3**, 597–612.
4. Iijima, S., Yudasaka, M., Yamada, R., Bandow, S., Suenaga, K., Kokai, F. *et al.*, Nano-aggregates of single-walled graphitec carbon nano-horns. *Chem. Phys. Lett.*, 1999, **309**, 165–170.
5. Bandow, S., Kokai, F., Takahashi, K., Yudasaka, M., Qin, L. C. and Iijima, S., Interlayer spacing anomaly of single-wall carbon nanohorn aggregate. *Chem. Phys. Lett.*, 2000, **321**, 514–519.
6. Adelene Nisha, J., Yudasaka, M., Bandow, S., Kokai, F., Takahashi, K. and Iijima, S., Adsorption and catalytic properties of single-wall carbon nanohorns. *Chem. Phys. Lett.*, 2000, **328**, 381–386.
7. Iijima, S., Carbon nanotubes: past, present, and future. *Physica B*, 2002, **323**, 1–5.
8. Takikawa, H., Ikeda, M., Hirahara, K., Hibi, Y., Tao, Y., Ruiz Jr., P. A. *et al.*, Fabrication of single-walled carbon nanotubes and nanohorns by means of a torch arc in open air. *Physica B*, 2002, **323**, 277–279.
9. Kokai, F., Takahashi, K., Kasuya, D., Yudasaka, M. and Iijima, S., Growth dynamics of single-wall carbon nanotubes and nanohorn aggregates by CO_2 laser vaporization at room temperature. *Appl. Surf. Sci.*, 2002, **197–198**, 650–655.
10. Oku, T., Hirano, T., Kuno, M., Kusunose, T., Niihara, K., Suganuma, K. *et al.*, Synthesis, atomic structures and properties of carbon and boron nitride fullerene materials. *Mater. Sci. Eng. B*, 2000, **74**, 206–217.
11. Oku, T., Narita, I., Nishiwaki, A. and Koi, N., Atomic structures, electronic states and hydrogen storage of boron nitride nanocage clusters, nanotubes and nanohorns. *Defect Diffus. Forum*, 2004, **226–228**, 113–140.
12. Kitahara, H. and Oku, T., Nanostruftures and electronic properties of carbon and boron nitride nanocapsules. *J. Ceram. Proc. Res.*, 2004, **5**, 89–93.
13. Mickelson, W., Aloni, S., Han, W.-Q., Cumings, J. and Zettl, A., Packing C_{60} in boron nitride nanotubes. *Science*, 2003, **300**, 467–469.
14. Golberg, D., Xu, F.-F. and Bando, Y., Filling boron nitride nanotubes with metals. *Appl. Phys. A*, 2003, **76**, 479–485.
15. Narita, I. and Oku, T., Effects of catalytic metals for synthesis of BN fullerene nanomaterials. *Diamond Relat. Mater.*, 2003, **12**, 1146–1150.
16. Oku, T. and Narita, I., Atomic structures and stabilities of zigzag and armchair-type boron nitride nanotubes studied by high-resolution electron microscopy and molecular mechanics calculation. *Diamond Relat. Mater.*, 2004, **13**, 1254–1260.
17. Oku, T., Hiraga, K., Matsuda, T., Hirai, T. and Hirabayashi, M., Formation and structures of multiply-twinned nanoparticles with fivelold symmetry in chemical vapor deposited boron nitride. *Diamond Relat. Mater.*, 2003, **12**, 1918–1926.
18. Oku, T., Hiraga, K., Matsuda, T., Hirai, T. and Hirabayashi, M., Twin structures of rhombohedral and cubic boron nitride prepared by chemical vapor deposition method. *Diamond Relat. Mater.*, 2003, **12**, 1138–1145.
19. Nishiwaki, A., Oku, T. and Suganuma, K., Atomic and electronic structures of endohedral $B_{36}N_{36}$ clusters with doping elements studied by molecular orbital calculations. *Physica B*, 2004, **349**, 254–259.
20. Golberg, D., Bando, Y., Stéphan, O. and Kurashima, K., Octahedral boron nitride fullerenes formed by electron beam irradiation. *Appl. Phys. Lett.*, 1998, **73**, 2441–2443.
21. Oku, T., Nishiwaki, A., Narita, I. and Gonda, M., Formation and structure of $B_{24}N_{24}$ clusters. *Chem. Phys. Lett.*, 2003, **380**, 620–623.
22. Oku, T., Nishiwaki, A. and Narita, I., Formation and atomic structures of B_nN_n ($n = 24$–60) clusters studied by mass spectrometry, high-resolution electron microscopy and molecular orbital calculations. *Physica B*, 2004, **351**, 184–190.
23. Golberg, D., Rode, A., Bando, Y., Mitome, M., Gamaly, E. and Luter-Davies, B., Boron nitride nanostructures formed by ultra-high-repetition rate laser ablation. *Diamond Relat. Mater.*, 2003, **12**, 1269–1274.
24. Nishiwaki, A., Oku, T. and Narita, I., Formation and atomic structure of boron nitride nanohorns. *Sci. Tech. Adv. Mater.*, 2004, **5**, 629–634.